JOURNAL OF Applied Polymer SCIENCE

Preparation and Dielectric Properties of Sulfonated Poly(aryl ether ketone)/Acidified Graphite Nanosheet Composites

Wenlong Jiang,[1] Yu Liu,[2] Jinfeng Wang,[3] Qitong Wang,[1] Yunhe Zhang,[1] Shaowei Guan[1]

[1]Alan G. MacDiarmid Laboratory, College of Chemistry, Jilin University, Changchun 130012, People's Republic of China

[2]Institute of Metal Research, Chinese Academy of Sciences, Shenyang 110016, People's Republic of China

[3]Australian Future Fibres Research & Innovation Centre, Institute for Frontier Materials, Deakin University, Geelong, Victoria 3217, Australia

Correspondence to: Y. Zhang (E-mail: zhangyuhe@jlu.edu.cn)

ABSTRACT: Percolative dielectric composites of sulfonated poly(aryl ether ketone) (SPAEK) and acidified graphite nanosheets (AGSs) were fabricated by a solution method. The dielectric constant of the as-prepared composite with 4.01 vol % AGSs was found to be 330 at 1000 Hz; this was a significant increase compared to that of pure SPAEK. Through the calculation, a low percolation threshold of the AGS/SPAEK composite was confirmed at 3.18 vol % (0.0318 volume fraction) AGSs; this was attributed to the large surface area and high conductivity of the AGSs. Additionally, our percolative dielectric composites also exhibited good mechanical performances and good thermostability, with a tensile strength of 71.7 MPa, a tensile modulus of 1.91 GPa, a breaking elongation of 16.4%, and a mass loss temperature at 5% of 336°C. © 2013 Wiley Periodicals, Inc. J. Appl. Polym. Sci. **2014**, *131*, 40028.

KEYWORDS: composites; dielectric properties; electrochemistry

Received 26 June 2013; accepted 29 September 2013
DOI: 10.1002/app.40028

INTRODUCTION

With the rapid development of the electronics industry, high-dielectric-constant materials under the effects of a good blocking carrier, energy-storage electricity, and a uniform electric field have very important applications. Although more and more studies have been performed to improve the electromechanical actuation and to examine the mechanism of the high dielectric constant,[1] numerous works have focused on the preparation of composites with good dielectric properties (high dielectric constant and low dielectric loss), excellent mechanical strength, and a low percolation threshold (f_c).

Poly(aryl ether ketone)s have achieved a remarkable position among other thermoplastic polymers because of their unique chemical stability, thermooxidative stability, mechanical properties at high temperatures, and radiant resistance. Sulfonated poly(aryl ether ketone) (SPAEK) had a special structure of ether and ketone bond that arrayed by turns and was similar to PAEK's. Not only could it make the composites possess higher intensity, but it also could retain its tenacity. Because of the side chain with a polarity sulfate group, it has a higher dielectric constant (~6.5 at 1000 Hz and room temperature) and has been used to prepare polymer-based dielectric percolative composites. For example, Liu et al.[2] prepared a series of SPAEK/acidified multiwalled carbon nanotubes (a-MWNTs) composites with high dielectric constants and low f_c. f_c of the a-MWNTs/SPAEK composites was only 3 vol % a-MWNTs, and the dielectric constant reached 210 (at 1000 Hz). The composite exhibited a higher dielectric constant, which was near 600 when the volume fraction of carbon nanotubes was 0.07 (7 vol %) at 1000 Hz and room temperature. Yang et al.[3] studied SPAEK/25 wt % copper phthalocyanine oligomer composites possessing a dielectric constant of 600 (tan $\delta < 0.5$) at 100 Hz. Ren et al.[4] investigated SPAEK/2,9,16,23-tetraaminophthalocyanine (4-NH_2-ZnPc) composites. In their study, the composites with 40 wt % 4-NH_2-ZnPc showed a dielectric constant of 23 (tan $\delta \approx 0.5$) at 100 Hz and room temperature. Zhang et al.[5] researched SPAEK/a-MWCNT–polyaniline composites, which exhibited a high dielectric constant above 800 and a tan δ of less than 1.1 at 10 kHz and room temperature.

Different types of graphite nanosheets (GNSs) forms, such as expanded graphite, exfoliated graphite, and graphene, have been used to make conductive nanocomposites. Expanded graphite reinforced with thermoplastics and thermosets have been studied by various researchers. This research has shown a substantial decrease in the critical GNS filler contents at f_c and a better distribution morphology compared to conventional fillers such as carbon black and flake graphite. In general, most of these studies have focused on the electrical or mechanical strength

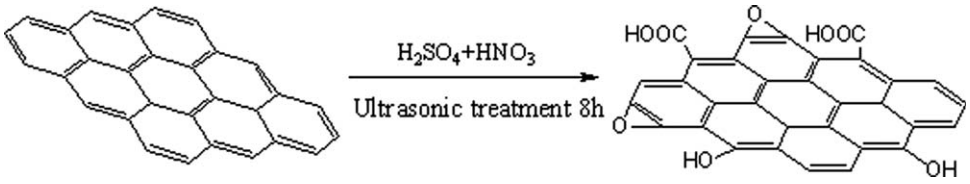

Scheme 1. Preparation of AGS.

properties of polymer/GNS nanocomposites,[6,7] whereas investigations into the dielectric properties of polymer/GNS composites have been deficient. For example, Min[8] investigated epoxy/GNS composites and found that the dielectric constant of composites with a 3.5 wt % graphite filler content reached 240 in the intermediate-frequency range and higher than 100 in the high-frequency range. Shang et al.[9] investigated the dielectric properties of GNS/poly(vinylidene fluoride) composites. A substantially increased dielectric constant of 63 was obtained at 100 Hz when the concentration of the GNSs was 1.27 vol %; this was nine times higher than that of pure poly(vinylidene fluoride). However, it is still a challenge to control the dielectric constants of polymer–GNS percolative composites in the vicinity of f_c because of the poor dispersion of GNSs within the polymer matrix. Here, we present a simple, wet-chemistry procedure for preparing acidified graphite nanosheet (AGS)/SPAEK composites with a high dielectric constant, good mechanical strength, and low f_c.

EXPERIMENTAL

Materials

N,N-Dimethylformamide was purchased from Tianjin Tiantai Fine Chemicals Co., Ltd. Natural flake graphite was purchased from Henan Xinlei Graphite Co., Ltd. The SPAEK polymers were prepared in our laboratory according to previously published protocols.[2,10]

Preparation of GNSs

Briefly, the natural flake graphite was dried at 80°C in a vacuum oven for 24 h. Then, it was added to a mixture consisting of concentrated sulfuric acid and concentrated nitric acid at a volume ratio of 4:1. The mixture was stirred for 12 h, and this was followed by sonication for 4 h. The mixture was then filtered and washed with distilled water and alcohol repeatedly to pH 6. The suspension was dried at 80°C *in vacuo* to form the graphite intercalation compound. The graphite intercalation compound was then rapidly expanded at 900°C for 15 s in a muffle furnace to form expanded

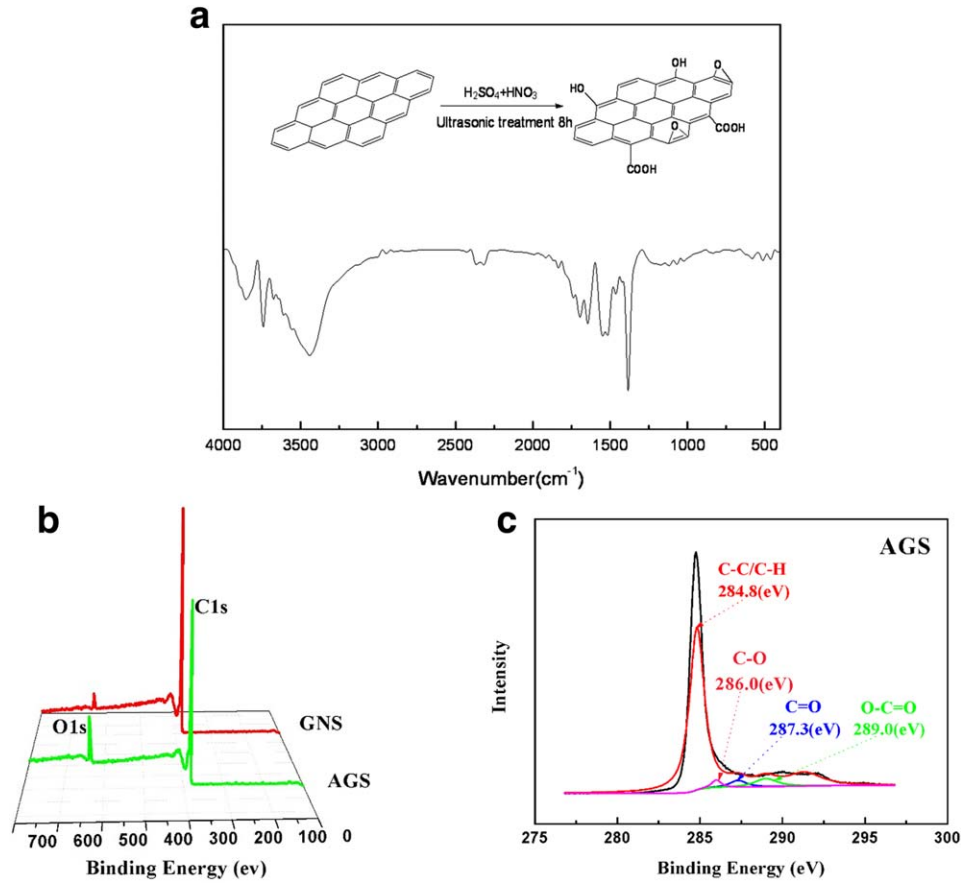

Figure 1. (a) FTIR spectrum of AGS, (b) XPS general spectra of GNS and AGS, and (c) high-resolution C1s spectra of AGS. [Color figure can be viewed in the online issue, which is available at wileyonlinelibrary.com.]

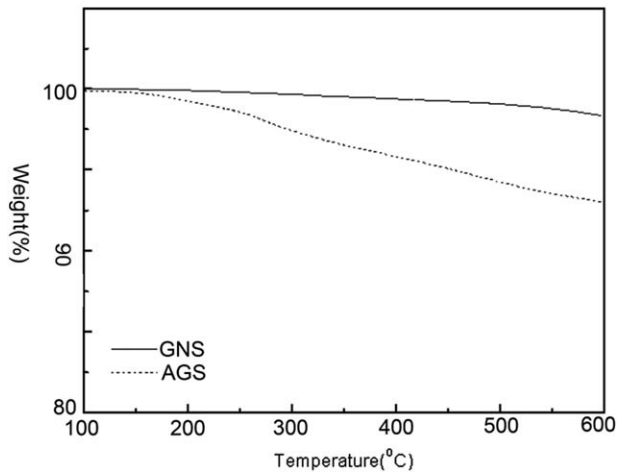

Figure 2. TGA curves of GNS and AGS.

graphite (EG). GNS was obtained by the sonication of the as-prepared EG.[11,12]

Preparation of AGSs

The GNSs was stirred in a sulfuric and nitric acid solution with a volume ratio of 3:1. The GNSs were acidified to AGSs, as shown in Scheme 1. The mixture was ultrasonicated for 8 h, and then, the mixture was stirred. The solution was poured into icy distilled water. Subsequently, the mixture was filtered and washed with distilled water until the scrubbing solution become neutral. The resulting black cake was dried at 80°C.

Preparation of the Composite Films

The AGSs were weighted and dispersed in *N*-methyl-2-pyrrolidone by ultrasonication to form a stable suspension. At the same time, SPAEK was also dissolved in *N*-methyl-2-pyrrolidone. Then, the previous two suspensions were mixed and then subjected to ultrasonication for 3 h. The mixture was stirred for 12 h to get a homogeneous suspension. The suspension was coated on the glass substrate, heated to 80°C for 24 h, and finally dried at 120°C for 24 h *in vacuo* to obtain the AGS/SPAEK composite membrane. GNS/SPAEK was prepared with the same procedure used for AGS/SPAEK.

Characterization

The Fourier transform infrared (FTIR) spectrum was recorded by a Nicolet Impact 410 FTIR spectrometer. The microstructures of the AGS/SPAEK composites were characterized with scanning electron microscopy (SEM; JEOL JSM-6700). To investigate the morphologies of the composites, they were broken in liquid nitrogen, and their cross sections were analyzed by SEM. X-ray diffraction (XRD) patterns were recorded with a Rigaku D/Max-2500 X-ray apparatus. The mechanical properties of the AGS/SPAEK composites were measured at room temperature on a Shimadzu AG-I 1KN at a strain rate of 2 mm/min; this required dumbbell-shaped samples. Thermogravimetric analysis (TGA) was performed in a nitrogen atmosphere with a heating ramp of 10°C/min. The dielectric response of the composites was measured with an Alph-A high-performance frequency analyzer, which demanded samples with an area of 1 cm^2 and two sides with a silver electrode, and the measurements were carried out in the frequency range of 10^2–10^6 Hz.

RESULTS AND DISCUSSION

Characteristics of the GNSs and AGSs

Acid treatment was used to introduce carboxyl groups, ether bonds, and hydroxyl groups, on the GNSs for better dispersion of the GNSs in solvent. The existence of carboxyl groups was characterized by FTIR spectroscopy, as shown in Figure 1(a). For the AGSs, the broad peak at 3433 cm^{-1} was attributed to the hydroxyl stretching vibrations of the C—OH groups, and the peaks at 1800 and 1500 cm^{-1} were assigned to the C=O stretching vibrations of typical carbonyl and carboxyl groups; this indicated the presence of —COOH functional groups.[13] A C—O—C band was also found at 1400–1000 cm^{-1}.[14] FTIR spectroscopy confirmed the acid modification of the GNSs. The X-ray photoelectron spectroscopy (XPS) results in Figure 1(b) showed that the oxygen concentration in the GNSs was only a small proportion, but after acidification, it drastically increased along with a reduction in the carbon content. The high-resolution core-level C1s spectra for the AGSs are presented in Figure 1(c), and this band indicated a considerable degree of oxidation with three major signatures corresponding to carbon atoms in different functional groups. The generation of oxygen functional groups, such as carbonyl groups, hydroxyls, epoxides,

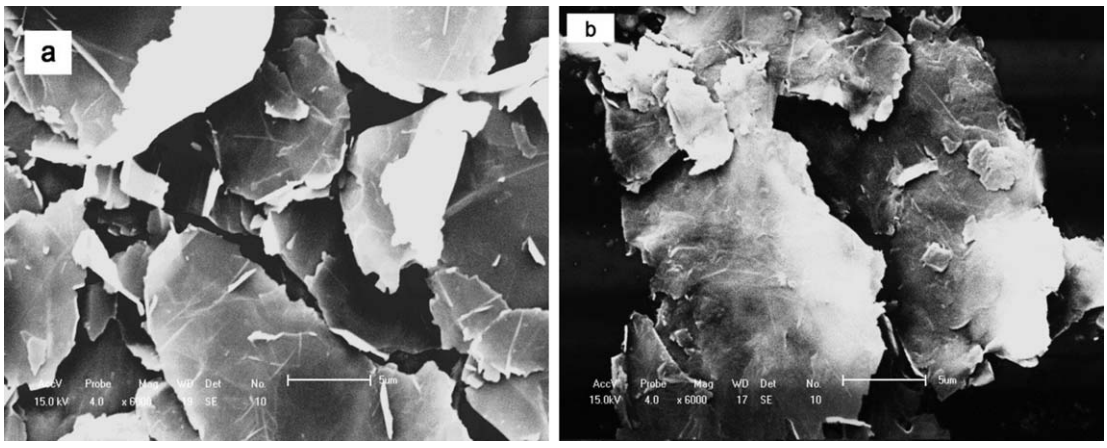

Figure 3. SEM images of (a) GNS and (b) AGS.

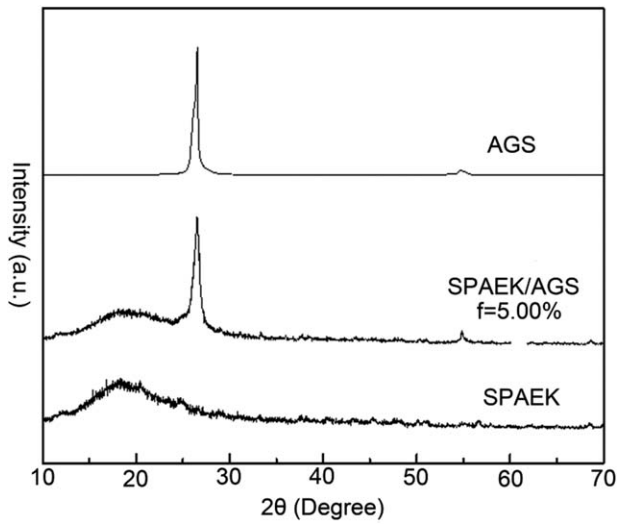

Figure 4. XRD of AGS, SPAEK, and AGS/SPAEK at f_{AGS} = 5.0%.

and carboxyls rendered the AGSs somewhat hydrophilic and more compatible with the polymer matrix. The XPS results also confirmed the acid modification of the GNSs.

Figure 2 shows the TGA curves of the GNSs and AGSs. There was almost no mass loss of the GNSs, which confirmed its good thermostability. For AGSs, weight loss started at 180°C and reached 5% at 450°C. This weight loss was attributed to the loss of carboxyl groups or ether bonds from surface of the AGSs. This result further confirmed the successful modification of the GNSs through acid treatment.

The SEM image of the GNSs shows that the size of GNSs ranged from 1 to 15 μm [Figure 3(a)]. The size of the GNSs was much smaller than that of the natural flake graphite, whose size was larger than 100 μm.[15] After the acid treatment, distinctive morphological changes were observed by SEM, as shown in Figure 3(b). Compared to the GNSs, the AGSs showed more ruffles on the surface and a smaller size.

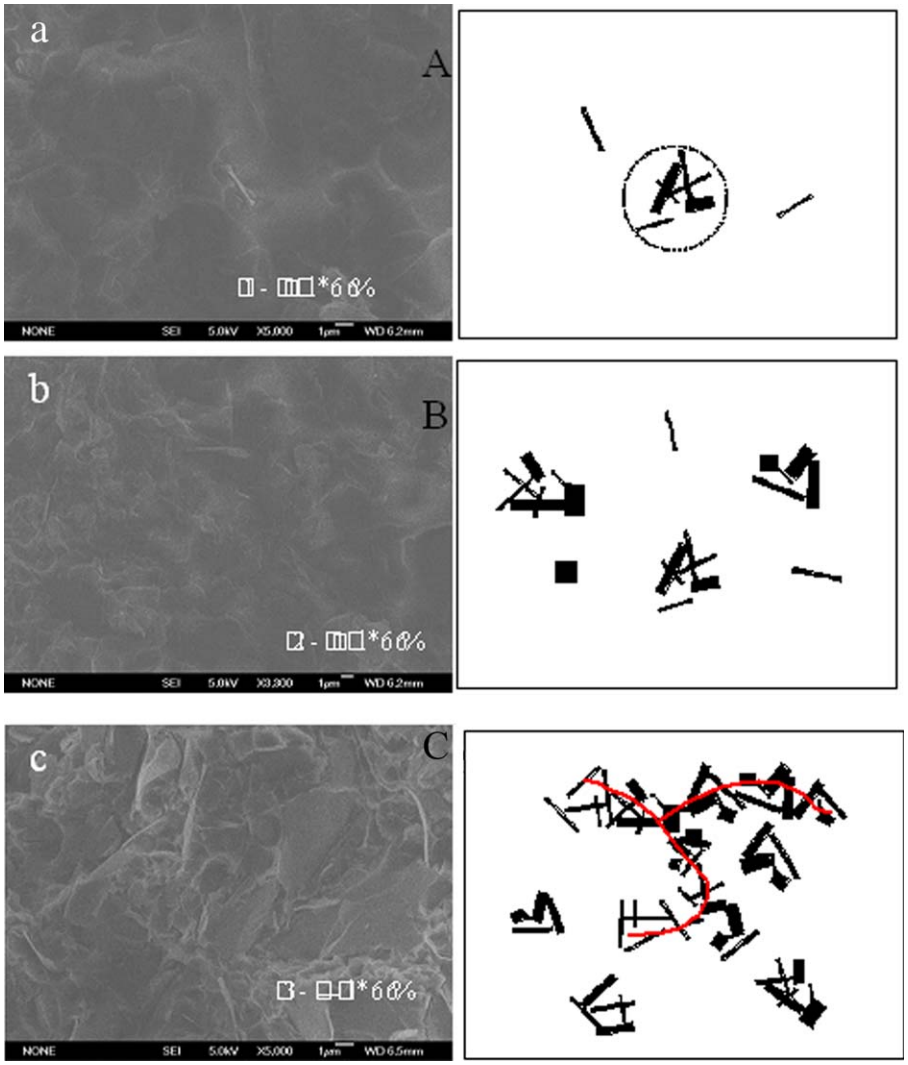

Figure 5. SEM images illustrating the morphology of sections of the AGS/SPAEK composites with AGS volume fractions of (a) 1.04, (b) 2.09, and (c) 3.18 vol %. Schematic pictures of the AGS distributions in the polymer composites with loading contents of (A) 1.04, (B) 2.09, and (C) 3.18 vol %. [Color figure can be viewed in the online issue, which is available at wileyonlinelibrary.com.]

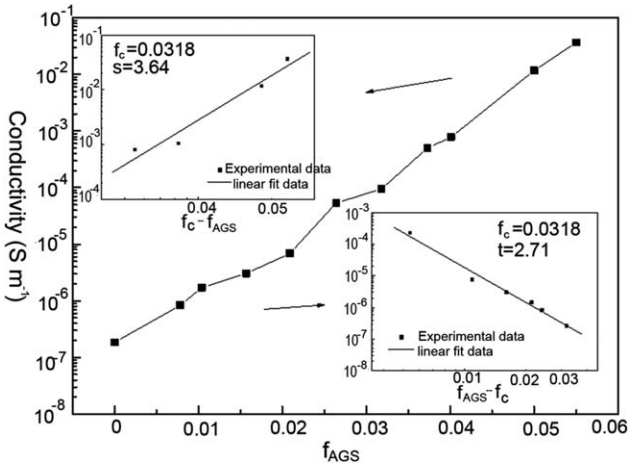

Figure 6. Alternating-current conductivity of the AGS/SPAEK composites versus the AGS volume fraction at room temperature and 1000 Hz. The insets show the best fits of eq. (1).

Characteristics of the AGS/SPAEK Composites

Figure 4 displays the XRD patterns of the AGSs, SPAEK, and AGS/SPAEK composites. For the AGSs, a characteristic peak of 2θ at 26.5° corresponding to the (002) diffraction was clearly detected.[16] The crystallization peak of the AGSs were still maintained after the combination with SPAEK confirmed that the crystal structure of the AGSs was not destroyed during the preparation of the AGS/SPAEK composite.

Micromorphologies and Mechanical Properties of the AGS/SPAEK Composites

AGS/SPAEK composites with AGS concentrations of 1.04, 2.09, and 3.18 vol % were fabricated. The surface morphologies of the previous AGS/SPEAK composites were characterized by SEM, as shown in Figure 5. The AGSs were well wrapped in the SPAEK matrix [Figure 5(a)] when the content of AGS was 1.04 vol %. The AGSs were detected on the fracture surfaces with increasing AGS loading contents [Figure 5(b,c)]. This may have been due to the aggregation of AGSs because of the π–π and hydrogen-bonding interactions. Schematic pictures of the AGS distribution in the polymer composites with different loadings are shown Figure 5(A–C), respectively. At low volume concentrations, the AGS clusters were wrapped by a polymer matrix; thus, a great number of tiny capacitors were formed within the SPAEK matrix. When the AGS volume concentration was increased, the AGS clusters could not be wrapped completely, and this resulted in the formation of AGS networks within the composites.

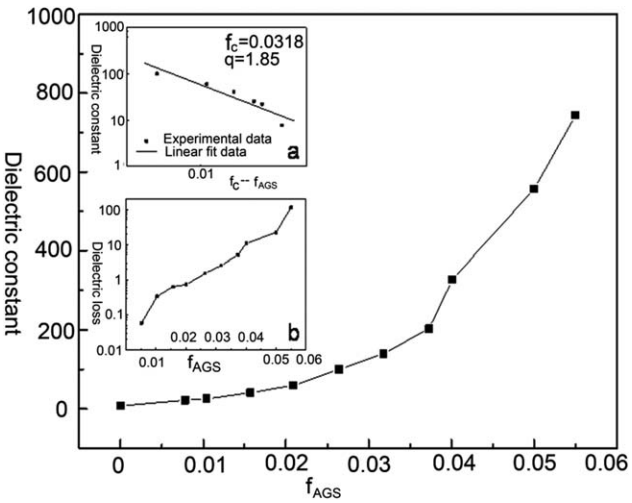

Figure 7. Dielectric constant of the AGS/SPAEK composites versus the AGS volume fraction at room temperature and 1000 Hz. The insets show the (a) best fits of eq. (3) and (b) dielectric loss of the AGS/SPAEK composites as a function of the AGS volume fraction.

Dielectric Properties of the AGS/SPAEK Composites

f_c is the critical fraction at which the conductivity increased significantly and the filler–polymer system transformed from being semiconductive to being conductive. The critical volume fraction at f_c was a key parameter for the percolative polymer-based composites. Figure 6 shows the alternating-current conductivity of the AGS/SPAEK composites as a function of the AGS volume fraction. An insulator–conductor translation at a filling content factor (f_{AGS}) of about 0.03–0.05 was observed, as shown in Figure 6. According to the percolation theory, the relation between the conducting filler content and the electrical conductivity of a composite [$\sigma(f_{AGS})$] in the vicinity of f_c can be defined by a simple power law:[17–20]

$$\sigma(f_{AGS}) \propto (f_c\text{-}f_{AGS})^{-s} \text{ for } f_{AGS} < f_c \quad (1)$$

$$\sigma(f_{AGS}) \propto (f_{AGS}\text{-}f_c)^{t} \text{ for } f_{AGS} > f_c \quad (2)$$

where s is the critical exponent in the insulating region and t is the critical exponent in the conducting region. The best fits of the electrical conductivity data to the log–log plots of the power laws gave f_c = 3.18 vol %, s = 3.64, and t = 2.71 according to eqs. (1) and (2), as shown in Figure 6.

Spherical or elliptical conducting fillers have been widely investigated in two-phase composites in which f_c was around 16 vol %;[2,21] this

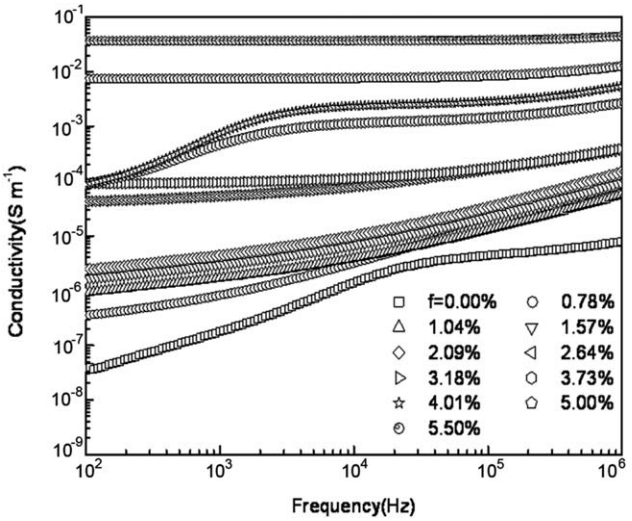

Figure 8. $\sigma(f_{AGS})$ as a function of the frequency at room temperature and f_{AGS} = 0–5.5 vol %.

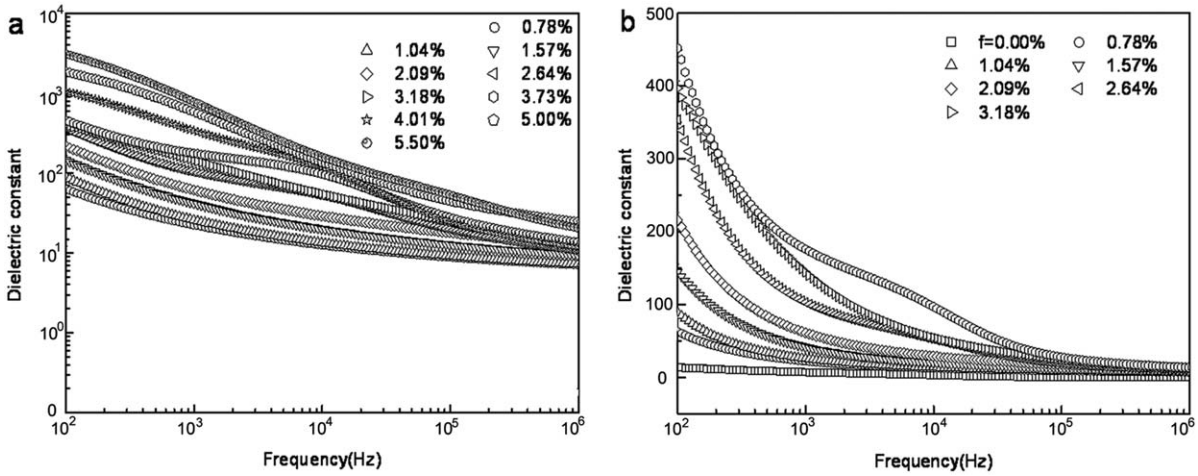

Figure 9. (a) Dielectric constant of the AGS/SPAEK composites as a function of frequency at room temperature and f_{AGS} = 0−5.5 vol % and (b) magnified image of panel a at f_{AGS} = 0−3.18 vol %.

value was much higher than that in the AGS/SPAEK composites (f_c = 3.18 vol %). Such a low f_c could be attributed to the higher aspect ratios of the AGSs compared to that of spherical or elliptical fillers, according to excluded volume theory.[22,23] Briefly, the more extreme the geometry of the filler particle is, the larger its excluded volume will be; the larger the excluded volume is, the lower f_c will be.

A large enhanced dielectric constant (135 at 1000 Hz) of the AGS/SPAEK composites was detected near f_c at room temperature; this was about 20 times higher than that of SPAEK (~6.5 at 1000 Hz; Figure 7). This variation of the dielectric constant [$\varepsilon(f_{AGS})$] near f_c is also given by a power law, as follows:[17,18,24]

$$\epsilon(f_{AGS}) \propto (f_c\text{-}f_{AGS})^{-q} \text{ for } f_{AGS} < f_c \quad (3)$$

where q is the dielectric critical exponent. The insert in Figure 7 shows the experimental value of the dielectric constant, which was in good agreement with eq. (3), with f_c = 3.18 vol % and q = 1.85. It was obvious that the AGS filler content might have played an important role in f_c of the AGS/SPAEK composites. This suggested that the increased concentration of AGS may have caused the formation of the conductive AGS networks in the AGS/SPAEK composites. The conductive AGS networks acted as minicapacitors in the composites and may have increased the dielectric constant of the AGS composites. Inset b in Figure 7 shows the dielectric loss of the AGS/SPAEK composites as a function of the AGS volume fraction. The loss tangent of AGS/SPAEK was observed to be 1.5 at its f_c. Tan δ increased remarkably with further increases in the AGS concentration in the composites; this may have resulted from the increased amount of conductive networks formed at high concentrations.

Figure 8 shows $\sigma(f_{AGS})$ as a function of the frequency at room temperature, with f_{AGS} ranging from 0 to 5.5 vol %, in the composites. The electrical conductivity increased with increasing AGS volume fraction and frequency. These results were consistent with those of previous studies.[25] At low concentrations, the conductivity increased significantly with increasing concentration. However, as the concentration was higher than f_c, the influence of the concentration on its conductivity became weaker and showed the typical gradual transformation of the AGS/SPAEK composites from being insulating to being conductive.

Figure 9 shows the dielectric constant of the AGS/SPAEK composites as a function of the frequency at room temperature with different AGS concentrations. When the volume fraction was 5.5 vol %, the dielectric constant of AGS/SPAEK was higher than 800 at 1000 Hz; this was 120 times larger than that of SPAEK. However, the dielectric constant decreased rapidly with increasing frequency. This phenomenon could be explained by the Maxwell–Wagner effect.[26] The large surface area of the AGSs provided strong interface polarization at the interface between the two phases; thus, strong interfacial polarization was generated at a low frequency,[27] and this resulted in a high dielectric constant at low frequencies. At high frequencies, the separation rates of the charges were lower than the increasing rate of the frequency and showed a weak influence on the electrical properties.

Mechanical Properties of the AGS/SPAEK Composites

The AGS/SPAEK composites showed better mechanical strength compared to SPAEK because of good interphase interaction between the SPAEK and AGSs. Table I lists the mechanical properties of the SPAEK and AGS/SPAEK composites with different concentrations of AGSs. The composite with 3.18 vol % AGSs showed a tensile strength of 71.7 MPa, a tensile modulus

Table I. Mechanical Properties of the SPAEK and AGS/SPAEK Composites with Different Concentrations of AGSs

Polymer	Tensile strength (MPa)	Young's modulus (GPa)	Elongation at break (%)
SPAEK	60.2	1.20	16.4
AGS/SPAEK (f = 3.18 vol %)	71.7	1.91	6.0
AGS/SPAEK (f = 5.50 vol %)	67.8	4.02	3.9

Note: f: volume fraction.

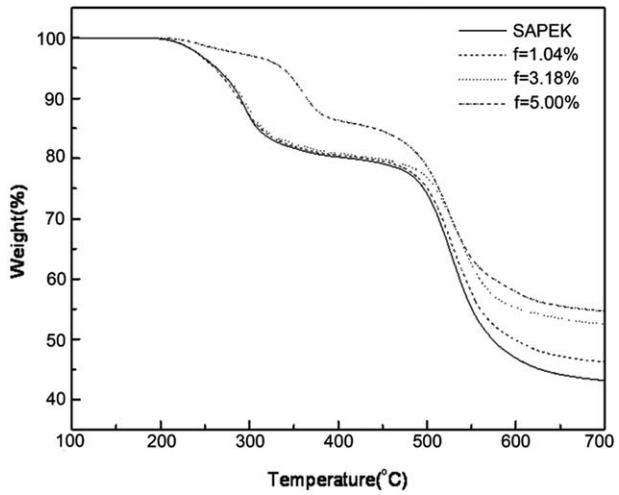

Figure 10. TGA curves of the AGS/SPAEK composites.

of 1.91 GPa, and a breaking elongation of 16.4%. A further increase in the concentration of AGSs diluted the polymer matric and resulted in a relative decrease in the mechanical properties. At 5.5 vol % AGSs, the tensile strength was 67.8 MPa, the modulus was 4.02 GPa, and the breaking elongation was 3.9%. With increasing AGS content in the composites, the Young's modulus increased, whereas the tensile strength first increased and then decreased. This was attributed to the counterbalance of the increased surface fracture energy and the increased sizes of the voids or AGS aggregates as the AGS content in the polymer composites increased.[28,29] Because dispersed AGS in the composites made the crack propagation path longer, absorbed a portion of the energy, and enhanced the plastic deformation, the surface fracture energy of the materials increased, and the strength of the composites should have increased as well as a function of the AGS contents.[29] However, with increasing AGS content, the size of the voids due to the detachment of SPAEK from the AGSs gradually increased and might have initiated the main crack.[29] In addition, the inevitably increased agglomeration of dispersed filler particles resulted in a decreased mechanical strength because of the low strength of the agglomerates themselves.[28]

Thermal Properties of the AGS/SPAEK Composites

Figure 10 shows the TGA curves of the SPAEK matrix and AGS/SPAEK composites with different AGS concentrations. From the curves, we observed that the mass loss of SPAEK started from 200°C; this was mainly caused by the disintegration of sulfonic groups on the side chain. The second mass loss above 300°C was initialized by the main-chain disintegration of SPAEK. For the AGS/SPAEK (f_{AGS} = 5.0 vol %) composites, 5% mass loss was observed at 336°C, and 14% weight loss was found at 366°C; this was compared to the 20% weight loss at 366°C for SPAEK. Therefore, the AGS/SPAEK composites showed better thermal stability than SPAEK.

CONCLUSIONS

In summary, novel AGS/SPAEK polymer-based composites were prepared via a solution-blending technique; they showed a high dielectric constant, excellent mechanical strength, and low f_c. We also studied the effects of the frequency and volume fraction of the AGSs on the dielectric properties of the AGS/SPAEK composites. The composites exhibited a higher dielectric constant, which was more than 800 at 1000 Hz and room temperature when the volume fraction was 5.5 vol %. f_c of the AGS/SPAEK composite was only 3.18 vol % (0.0318 volume fraction) that of the AGSs because of the large specific surface area and the high conductivity of the AGSs.

ACKNOWLEDGMENTS

This work was financially supported by the National Nature Science Foundation of China (contract grant number 51203172).

REFERENCES

1. Dang, Z. M.; Yao, S. H.; Xu, H. P. *Appl. Phys. Lett.* **2007**, *90*, 012907.
2. Liu, X.; Zhang, Y. H.; Zhu, M.; Yang, X.; Rong, C. R.; Wang, G. B. *Soft Mater.* **2011**, *9*, 94.
3. Yang, Y.; Wang, Q. T.; Zhang, Y. H.; Jiang, Z. H. *Polym. J.* **2012**, *44*, 1042.
4. Ren, D. F.; Wei, W. W.; Jiang, Z. H.; Zhang, Y. H. *Polym.-Plast. Technol. Eng.* **2012**, *51*, 1372.
5. Zhang, Y. H.; Huo, P. F.; Wang, J. F.; Liu, X.; Rong, C. R.; Wang, G. B. *J. Mater. Chem. C* **2013**, *1*, 4035.
6. Wang, L.; Chen, G. *J. Appl. Polym. Sci.* **2010**, *116*, 2029.
7. Yang, X.; Zhan, Y.; Zhao, R.; Liu, X. *J. Appl. Polym. Sci.* **2012**, *124*, 1723.
8. Min, C.; Yu, D. M. *Polym. Eng. Sci.* **2010**, *50*, 1734.
9. Shang, J.; Zhang, Y.; Yu, L.; Luan, X.; Shen, B.; Zhang, Z.; Lv, F.; Chu, P. K. *J. Mater. Chem. A* **2013**, *1*, 884.
10. Zhang, Y. H.; Huo, P. F.; Liu, X.; Rong, C. R.; Wang, G. B. *J. Appl. Polym. Sci.* **2013**, *130*, 1990.
11. Pan, Y. X.; Yu, Z. Z.; Ou, Y. C.; Hu, G. H. *J. Polym. Sci. Part B: Polym. Phys.* **2000**, *38*, 1126.
12. Potts, J. R.; Dreyer, D. R.; Bielawski, C. W.; Ruoff, R. S. *Polymer* **2011**, *52*, 5.
13. Mawhinney, D. B.; Yates, J. T. *Carbon* **2001**, *39*, 1167.
14. Elzein, T.; Nasser-Eddine, M.; Delaite, C.; Bistac, S.; Dumas, P. *J. Colloid Interface Sci.* **2004**, *273*, 381.
15. Wang, Q. T.; Jiang, W. L.; Guan, S. W.; Zhang, Y. H. *J. Inorg. Organomet. Polym. Mater.* **2013**, *23*, 743.
16. Weng, W. G.; Chen, G. H.; Wu, D. J.; Lin, Z. Y.; Yan, W. L. *Synth. Met.* **2003**, *139*, 221.
17. Dang, Z. M.; Nan, C. W.; Xie, D.; Zhang, Y. H.; Tjong, S. C. *Appl. Phys. Lett.* **2004**, *85*, 97.
18. Nan, C. W. *Prog. Mater. Sci.* **1993**, *37*, 1.
19. Kilbride, B. E.; Coleman, J. N.; Fraysse, J.; Fournet, P.; Cadek, M.; Drury, A.; Hutzler, S.; Roth, S.; Blau, W. J. *J. Appl. Phys. Lett.* **2002**, *92*, 4024.
20. Kirpatrick, S. *Rev. Mod. Phys.* **1973**, *45*, 574.

21. Wang, L.; Dang, Z. M. *Appl. Phys. Lett.* **2005**, *87*, 042903.
22. Balberg, I.; Anderson, C. H.; Alexander, S.; Wagner, N. *Phys. Rev.* **1984**, *30*, 3933.
23. Balberg, I.; Binenbaum, N.; Wagner, N. *Phys. Rev. Lett.* **1984**, *52*, 1465.
24. Dang, Z. M.; Lin, Y. H.; Nan, C. W. *Adv. Mater.* **2003**, *15*, 1625.
25. Nan, C. W. *Prog. Mater. Sci.* **1993**, *37*, 1.
26. Li, Y. C.; Tjong, S. C.; Li, R. K. Y. *Synth. Met.* **2010**, *160*, 1912.
27. Fan, B. H.; Zha, J. W.; Wang, D.; Zhao, J.; Dang, Z. M. *Appl. Phys. Lett.* **2012**, *100*, 012903.
28. Nielsen, L. E. Mechanical Properties of Polymers and Composites; Marcel Dekker: New York, **1974**; Vol.*1*.
29. Berlin, A. A.; Volfson, S. A.; Enikolopian, N. S.; Negmatov, S. S. Principles of Polymer Composites; Springer: Berlin, **1986**; Vol.*10*, p 124.